ISSN 0036-0295, Russian Metallurgy (Metally), Vol. 2017, No. 2, pp. 127–135. © Pleiades Publishing, Ltd., 2017.
Original Russian Text © D.V. Alexandrov, G.Yu. Dubovoi, A.P. Malygin, I.G. Nizovtseva, L.V. Toropova, 2017, published in Rasplavy, 2017, No. 1, pp. 3–17.

Solidification of Ternary Systems with a Nonlinear Phase Diagram

D. V. Alexandrov*, G. Yu. Dubovoi, A. P. Malygin, I. G. Nizovtseva, and L. V. Toropova

Ural Federal University, ul. Mira 19, Yekaterinburg, 620002 Russia

**e-mail: Dmitri.Alexandrov@urfu.ru*

Received September 7, 2016; in final form, September 8, 2016

Abstract—The directional solidification of a ternary system with an extended phase transition region is theoretically studied. A mathematical model is developed to describe quasi-stationary solidification, and its analytical solution is constructed with allowance for a nonlinear liquidus line equation. A deviation of the liquidus equation from a linear function is shown to result in a substantial change in the solidification parameters.

Keywords: solidification, mushy zone, nonlinear phase diagram

DOI: 10.1134/S0036029517020021

INTRODUCTION

Melt solidification often occurs in the presence of a long phase transition region (two-phase, or mushy, zone), which appears due to a thermal or concentration supercooling [1–3]. The processes of new-phase nucleation and growth take place in this supercooled zone and are accompanied by the release of the latent heat of solidification [4–7]. If this heat compensates for the supercooling, the mushy zone is called quasi-equilibrium [1, 2, 8–10]. The authors of [11, 12] were the first to develop a mathematical model for the mushy zone, and analytical solutions to this model, which describe the real processes of solidification of binary systems under quasi-stationary and nonstationary conditions, were found in [13–16] and [17–19], respectively.

However, the simulation of solidification using a binary system the concentration of which describes all solutes cannot always be performed. The influence of the main impurity and other components should often be taken into account to describe the solidification of a multicomponent solution. If the second dominating component can be distinguished among them, this situation corresponds to a ternary system. Based on the experimental data from [21], Andersen [20] proposed a mathematical model to describe the directional solidification of ternary systems with a linear phase diagram. The authors of [22] and [23, 24] then found its exact analytical solutions under quasi-stationary and self-similar solidification conditions, respectively.

The experimental and theoretical studies [25–27] showed that the nonlinearity of a phase diagram can radically change the solidification characteristics. For example, we [26] studied binary systems and showed that, when the nonlinearity of a phase diagram is taken into account, the mushy zone length increases more than twofold (as compared to the linear phase diagram). In this work, we continue to study the solidification of ternary systems and investigate the influence of the nonlinearity of a phase diagram on directional solidification.

MODEL FOR THE DIRECTIONAL SOLIDIFICATION OF A TERNARY SYSTEM

We consider the directional solidification of a ternary system along spatial axis z (Fig. 1) Let B and C be the concentrations of two substances dissolved in solvent A ($A + B + C = 1$). Since the parent substance undergoes a phase transition in the region that does not coincide with the phase transition region of the second substance, two two-phase zones, namely, parent and cotectic zones, appear during solidification. Let their lengths be δ_P and δ_C. Since the phase diagram of this system was discussed in detail in [20, 22–24], we will not dwell on liquidus, cotectic, and eutectic equations and refer the reader to those investigations. It is important that the relaxation time of the temperature field $\tau_T \sim l^2/\kappa$ is much shorter than the characteristic relaxation times of concentration fields $\tau_B \sim l^2/D_B$ and $\tau_C \sim l^2/D_C$, i.e., $\tau_T \ll \tau_C$ and $\tau_T \ll \tau_B$. Here, l is the characteristic length scale; κ is the thermal diffusivity; and D_B and D_C are the diffusion coefficients of impurity components B and C, respectively. As follows from this estimate of the relaxation time, the derivatives of temperature with respect to time t are much smaller than the other terms of the corresponding model equations. Allowing for this circumstance, we write a

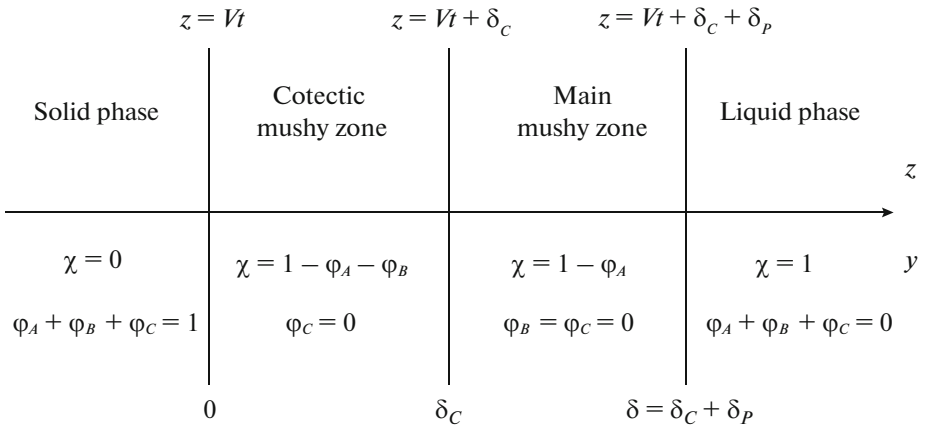

Fig. 1. Schematic diagram of the directional solidification of a ternary system with two phase transition regions.

mathematical model for the process using the results from [22–24].

In the liquid phase of the system (melt), impurity concentrations B_∞ and C_∞ and temperature gradient G_L are given,

$$B \to B_\infty, \quad C \to C_\infty, \quad z \to \infty, \tag{1}$$

$$\frac{\partial T}{\partial z} = G_L, \quad z > Vt + \delta = Vt + \delta_C + \delta_P, \tag{2}$$

where T is the temperature and V is the constant solidification rate. Moreover, the following impurity diffusion equations are fulfilled in the liquid phase:

$$\frac{\partial B}{\partial t} = D_B \frac{\partial^2 B}{\partial z^2}, \quad \frac{\partial C}{\partial t} = D_C \frac{\partial^2 C}{\partial z^2}, \quad z > Vt + \delta. \tag{3}$$

The boundary conditions at the main mushy zone–melt interface, which have the physical meaning of heat and mass balance and continuity conditions, are written as follows:

$$\begin{gathered} L_V V [\varphi_A]_-^+ = \left[\bar{k} \frac{\partial T}{\partial z}\right]_-^+, \\ [T]_-^+ = [B]_-^+ = [C]_-^+ = 0, \quad z = Vt + \delta, \end{gathered} \tag{4}$$

$$\begin{gathered} BV [\varphi_A]_-^+ = D_B \left[\chi \frac{\partial B}{\partial z}\right]_-^+, \\ CV [\varphi_A]_-^+ = D_C \left[\chi \frac{\partial C}{\partial z}\right]_-^+, \quad z = Vt + \delta. \end{gathered} \tag{5}$$

Here, L_V is the latent heat of solidification; $\bar{k} = k_L\chi + k_S(1 - \chi)$; k_L and k_S are the thermal conductivities of the melt and the solid phase, respectively; χ is the fraction of the liquid phase; and φ_A is the fraction of the solid phase of component A. Symbol $[\cdot]_-^+$ indicates the jump of the corresponding quantity at the boundary.

In the main mushy zone (where component A undergoes a phase transition ($\chi = 1 - \varphi_A$)), heat-and-mass transfer equations are written as

$$\begin{gathered} \frac{\partial}{\partial z}\left(\bar{k} \frac{dT}{dz}\right) + L_V \frac{\partial \varphi_A}{\partial t} = 0, \\ T = T_M + m_B B + m_C C + n_C C^2, \\ Vt + \delta_C < z < Vt + \delta, \end{gathered} \tag{6}$$

$$\begin{gathered} D_B \frac{\partial}{\partial z}\left(\chi \frac{\partial B}{\partial z}\right) - \frac{\partial}{\partial t}(\chi B) = 0, \\ D_C \frac{\partial}{\partial z}\left(\chi \frac{\partial C}{\partial z}\right) - \frac{\partial}{\partial t}(\chi C) = 0, \\ Vt + \delta_C < z < Vt + \delta, \end{gathered} \tag{7}$$

where T_M is the phase-transition temperature of the pure substance and m_B and m_C are the slopes of the liquidus equation.

We now write boundary conditions at the second interface between the cotectic and the main two-phase zones. These conditions reflect the heat and mass balance and the continuity of the temperature field and the impurity concentration fields and are written in the form [20, 22–24]

$$\begin{gathered} L_V V [\varphi_A + \varphi_B]_-^+ = \left[\bar{k} \frac{\partial T}{\partial z}\right]_-^+, \\ [T]_-^+ = [B]_-^+ = [C]_-^+ = 0, \end{gathered} \tag{8}$$

$$B = B^C(T), \quad C = C^C(T), \quad z = Vt + \delta_C, \tag{9}$$

$$\begin{gathered} V\left\{B[\varphi_A]_-^+ + (B-1)[\varphi_B]_-^+\right\} = D_B \left[\chi \frac{\partial B}{\partial z}\right]_-^+, \\ VC [\varphi_A + \varphi_B]_-^+ = D_C \left[\chi \frac{\partial C}{\partial z}\right]_-^+, \quad z = Vt + \delta_C, \end{gathered} \tag{10}$$

where φ_B is the fraction of the solid phase of component B.

Then, heat-and-mass transfer equations in the cotectic mushy zone, where components A and B ($\chi = 1 - \varphi_A - \varphi_B$) undergo a phase transition, are written as

$$\frac{\partial}{\partial z}\left(\bar{k}\frac{\partial T}{\partial z}\right) + L_V\frac{\partial(\varphi_A + \varphi_B)}{\partial t} = 0, \quad Vt < z < Vt + \delta_C, \tag{11}$$

$$B = B^C(T) = \frac{T_E + m_B^C B_E - T}{m_B^C}, \quad T = T_E^{AB} - m_C^C C + n_C^C C^2, \quad Vt < z < Vt + \delta_C, \tag{12}$$

$$D_B\frac{\partial}{\partial z}\left(\chi\frac{\partial B}{\partial z}\right) - \frac{\partial}{\partial t}(\chi B + \varphi_B) = 0,$$
$$D_C\frac{\partial}{\partial z}\left(\chi\frac{\partial C}{\partial z}\right) - \frac{\partial}{\partial t}(\chi C) = 0, \quad Vt < z < Vt + \delta_C, \tag{13}$$

where T_E, B_E, and C_E are the known temperature and the impurity concentrations at the eutectic point of the ternary system, respectively, and T_E^{AB} is the temperature at the eutectic point of the binary system.

The boundary conditions at the surface between the solid phase and the cotectic zone have the form

$$L_V V\left[\varphi_A + \varphi_B + \varphi_C\right]_-^+ = \left[\bar{k}\frac{\partial T}{\partial z}\right]_-^+, \quad z = Vt, \tag{14}$$

$$V\left\{B\left[\varphi_A\right]_-^+ + (B-1)\left[\varphi_B\right]_-^+ + B\left[\varphi_C\right]_-^+\right\} = D_B\left[\chi\frac{\partial B}{\partial z}\right]_-^+, \quad z = Vt, \tag{15}$$

$$V\left\{C\left[\varphi_A\right]_-^+ + C\left[\varphi_B\right]_-^+ + (C-1)\left[\varphi_C\right]_-^+\right\} = D_C\left[\chi\frac{\partial C}{\partial z}\right]_-^+, \quad z = Vt. \tag{16}$$

In the solid phase, we have a constant temperature gradient G_S, i.e.,

$$\frac{\partial T}{\partial z} = G_S, \quad z < Vt. \tag{17}$$

The set of Eqs. (1)–(17) is a closed system of equations and boundary conditions for searching for the solution to the problem of the solidification of a ternary melt at a constant rate.

METHOD FOR SOLVING THE NONLINEAR MODEL

We now pass to the coordinate system moving at constant velocity V. In this new coordinate system, solidification is a steady process and all unknown functions are time-independent.

Diffusion equations (3) under boundary conditions (1) have the following integrals:

$$B(y) = B_\infty + B_1\exp\left(\frac{-Vy}{D_B}\right),$$
$$C(y) = C_\infty + C_1\exp\left(\frac{-Vy}{D_C}\right), \quad y > \delta = \delta_C + \delta_P, \tag{18}$$

where B_1 and C_1 are the constants of integration. Integrating heat-and-mass transfer equations (6) and (7) in the main mushy zone, we find the derivatives of the impurity temperature and concentration,

$$\frac{dT}{dy} = \frac{(L_V V\varphi_A + A_1)}{\bar{k}_P(\varphi_A)}, \quad \bar{k}_P(\varphi_A) = k_L(1-\varphi_A) + k_S\varphi_A, \quad \delta_C < y < \delta, \tag{19}$$

$$\frac{dB}{dy} = \frac{A_2 - BV(1-\varphi_A)}{D_B(1-\varphi_A)},$$
$$\frac{dC}{dy} = \frac{A_3 - CV(1-\varphi_A)}{D_C(1-\varphi_A)}, \quad \delta_C < y < \delta, \tag{20}$$

where $A_1 = \bar{k}_P\left(\varphi_{APL}^-\right)G_{PL} - VL_V\varphi_{APL}^-$, A_2, and A_3 are constants of integration and G_{PL} and φ_{APL}^- the temperature gradient and the fraction of the solid phase at $y = \delta$ determined on the side of the main mushy zone. These unknowns will be found later. When combining Eqs. (19) and (20) with liquidus equation (6), we determine the relation between the B and C concentrations in the main mushy zone,

$$B(\varphi_A) = g(\varphi_A) - \frac{D_B m_C}{D_C m_B}C(\varphi_A) + \frac{2A_3 n_C D_B}{Vm_B D_C(1-\varphi_A)}C(\varphi_A) - \frac{2n_C D_B}{m_B D_C}C^2(\varphi_A),$$
$$\delta_C < y < \delta, \quad g(\varphi_A) = \frac{D_B}{Vm_B}\left[\frac{m_B A_2}{D_B(1-\varphi_A)} + \frac{m_C A_3}{D_C(1-\varphi_A)} - \frac{\left(L_V V(\varphi_A - \varphi_{A_{PL}}^-) + \bar{k}_P\left(\varphi_{A_{PL}}^-\right)G_{PL}\right)}{\bar{k}_P(\varphi_A)}\right]. \tag{21}$$

From Eq. (20), we find the dependence $\frac{dB}{dC}$ in the main mushy zone,

$$\frac{dB}{dC} = \frac{(A_2 - VB(1-\varphi_A))D_C}{(A_3 - VC(1-\varphi_A))D_B}. \tag{22}$$

We now consider the case $D_B \neq D_C$. We find dB from Eq. (21) and substitute it into Eq. (22). As a result, we obtain the expression

$$\frac{dC}{d\varphi_A} = \left[\frac{-2A_3 D_b n_C}{V m_B (1-\varphi_A) D_C g'(\varphi_A)} + \frac{m_C D_B}{m_B D_C g'(\varphi_A)} + \frac{4 n_C D_B C}{m_B D_C g'(\varphi_A)} + \frac{D_C \left(A_2 - V(1-\varphi_A) \left[g(\varphi_A) + C \left(\frac{2A_3 n_C D_B}{V m_B D_C (1-\varphi_A)} - \frac{m_C D_B}{m_B D_C} \right) - \frac{2 n_C D_B}{m_B D_C} C^2 \right] \right)}{D_B (A_3 - VC(1-\varphi_A)) g'(\varphi_A)} \right]^{-1}. \quad (23)$$

Relationship (23) is a differential equation. A boundary condition for solving this equation will be derived later from Eq. (10). Finding function $C(\varphi_A)$ in the main mushy zone, we obtain an expression for the other unknowns. Combining Eqs. (20) and (23), we obtain the dependence of the coordinate on the fraction of the solid phase and the mushy zone thickness,

$$y(\varphi_A) = \delta_C + \int_{\varphi^+_{A_{CP}}}^{\varphi_A} \frac{dC}{d\varphi_A} \frac{D_C(1-\varphi_A)}{A_3 - VC(1-\varphi_A)} d\varphi_A, \quad (24)$$

$$\delta = \delta_C + \delta_P = \delta_C + \int_{\varphi^+_{A_{CP}}}^{\varphi^-_{A_{PL}}} \frac{dC}{d\varphi_A} \frac{D_C(1-\varphi_A)}{A_3 - VC(1-\varphi_A)} d\varphi_A. \quad (25)$$

Equations (21)–(25) represent the parametric solution to the problem in the main mushy zone. Here, the fraction of the solid phase φ_A (or $\chi = 1 - \varphi_A$) of the component solidifying in this zone is a parameter.

Substituting the found solutions into conditions (4) and (5), we derive the following equations, which determine the unknown constants:

$$G_L = \frac{-m_B V B_1}{D_B} \exp\left(-\frac{V\delta}{D_B}\right) - \frac{m_C V C_1}{D_C} \exp\left(-\frac{V\delta}{D_C}\right) + 2n_C \left(C_\infty + C_1 \exp\left(-\frac{V\delta}{D_C}\right) \right) \left(\frac{VC_1}{D_C} \exp\left(-\frac{V\delta}{D_C}\right) \right), \quad (26)$$

$$G_{PL} = \frac{k_L G_L + L_V V \varphi^-_{APL}}{\bar{k}_P \left(\varphi^-_{APL} \right)}, \quad A_2 = VB_\infty, \quad A_3 = VC_\infty, \quad (27)$$

$$B_1 = \exp\left(\frac{V\delta}{D_B}\right) \left[g\left(\varphi^-_{A_{PL}}\right) - B_\infty + \left(\frac{2A_3 n_C D_B}{V m_B D_C (1-\varphi^-_{A_{PL}})} - \frac{m_C D_B}{m_B D_C} \right) \left(C_\infty + C_1 \exp\left(-\frac{V\delta}{D_C}\right) \right) - \frac{2 n_C D_B}{m_B D_C} \left(C_\infty + C_1 \exp\left(-\frac{V\delta}{D_C}\right) \right)^2 \right], \quad (28)$$

$$C_\infty + C_1 \exp\left(-\frac{V\delta}{D_C}\right) = C(\varphi^-_{APL}). \quad (29)$$

We now solve the problem in the cotectic zone. Integrating Eqs. (11) and (13) one time, we obtain the expressions

$$D_B \chi \frac{dB}{dy} + VB\chi + V\varphi_B = A_6, \; D_c \chi \frac{dC}{dy} + VC\chi = A_7, \quad (30)$$

$$\frac{dT}{dy} = \frac{\bar{k}_C(\chi^+_{SC}) G_{SC} - VL_V(1-\chi^+_{SC}) + VL_V(1-\chi)}{\bar{k}_C(\chi)} \equiv F_0(\chi). \quad (31)$$

Differentiating Eq. (12), we find the relation between $\frac{dB}{dy}$, $\frac{dC}{dy}$, and $\frac{dT}{dy}$. Substituting Eqs. (30) and (31) into these relations, we derive the following expressions for $\varphi_B(\chi)$, $\varphi_A(\chi)$, and $C(\chi)$:

$$\varphi_B(\chi) = \frac{D_B \chi}{m_B^C V} F_0(\chi) + \frac{A_6}{V} - \chi B(\chi), \quad \varphi_A(\chi) = 1 - \chi - \varphi_B(\chi), \quad (32)$$

$$C^2(\chi) \left(\frac{-2Vn_C^C}{D_C} \right) + C(\chi) \left(\frac{Vm_C^C}{D_C} + \frac{2n_C^C A_7}{D_C \chi} \right) - \left(\frac{m_C^C A_7}{D_C \chi} + F_0(\chi) \right) = 0. \quad (33)$$

Combining Eqs. (12), we find the relationship

$$B(\chi) = \frac{-n_C^C}{m_B^C} C^2(\chi) + m_{CB}^C C(\chi) + B_E + \frac{T_E - T_E^{AB}}{m_B^C}. \quad (34)$$

Note that only one of the two solutions to Eq. (33) lies in a unit segment. Plotting both solutions, we choose only one of them, namely, the physically allowed solution

$$C(\chi) = \frac{\frac{Vm_C^C}{D_C} + \frac{2n_C^C A_7}{D_{C\chi}} - \sqrt{\left(\frac{Vm_C^C}{D_C} + \frac{2n_C^C A_7}{D_{C\chi}}\right)^2 - 4\frac{2Vn_C^C}{D_C}\frac{m_C^C A_7}{D_{C\chi}} - 4\frac{2Vn_C^C}{D_C}F_0(\chi)}}{\frac{4Vn_C^C}{D_C}}. \quad (35)$$

Equation (31) is used to obtain the dependence of the coordinate on the fraction of the liquid phase and the cotectic two-phase zone thickness,

$$y(\chi) = \int\limits_{\chi_{SC}^+}^{\chi} \frac{dT}{d\chi}\frac{1}{F_0(\chi)}d\chi, \quad (36)$$

$$\delta_C = \int\limits_{\chi_{SC}^+}^{\chi_{CP}^-} \frac{dT}{d\chi}\frac{1}{F_0(\chi)}d\chi. \quad (37)$$

The solutions in the cotectic two-phase zone have been found. Substituting these solutions into boundary conditions (14)–(16) and taking into account temperature gradient (17), we obtain the following relationships for the unknown constants:

$$G_{SC} = \frac{k_S G_S - L_V V\chi_{SC}^+}{\bar{k}_C\left(\chi_{SC}^+\right)},$$
$$V\left(\varphi_{BSC}^- - \varphi_{BSC}^+ - B_E\chi_{SC}^+\right) + V\left(B_E\chi_{SC}^+ + \varphi_{BSC}^+\right) = A_6, \quad (38)$$

$$V\left(\varphi_{CSC}^- - \varphi_{CSC}^+ - C_E\chi_{SC}^+\right) + VC_E\chi_{SC}^+ = A_7, \quad (39)$$

$$A_7 = \frac{(G_{SC}D_C + 2C_E^2 Vn_C^C - C_E Vm_C^C)\chi_{SC}^+}{2n_C^C C_E - m_C^C}, \quad (40)$$

where φ_{BSC}^- and φ_{BSC}^+ are the fractions of the solid phase of component B to the left and right of the solid phase–cotectic zone boundary, respectively, and φ_{CSC}^- and φ_{CSC}^+ are the corresponding fractions for component C. Substituting the expressions found earlier into boundary conditions (9) and (10), we obtain

$$V = \frac{k_S G_S - k_L G_L}{L_V}, \quad A_6 = A_2 = VB_\infty, \quad (41)$$

$$A_7 = A_3 = VC_\infty, \quad (42)$$

$$C_{CP} = \frac{\frac{Vm_C^C}{D_C} + \frac{2n_C^C A_7}{D_C\chi_{CP}^-} - \sqrt{\left(\frac{Vm_C^C}{D_C} + \frac{2n_C^C A_7}{D_C\chi_{CP}^-}\right)^2 - 4\frac{2Vn_C^C}{D_C}\frac{m_C^C A_7}{D_C\chi_{CP}^-} - 4\frac{2Vn_C^C}{D_C}F_0(\chi_{CP}^-)}}{\frac{4Vn_C^C}{D_C}}, \quad (43)$$

$$B_\infty - (1-\varphi_{A_{CP}}^+)\left[B^* - \frac{n_C^C}{m_B^C}C_{CP}^2 + m_{CB}^C C_{CP}\right]$$
$$= m_{CB}^C D_{BC}\left(C_\infty - C_{CP}(1-\varphi_{A_{CP}}^+)\right)$$
$$- 2\frac{n_C^C}{m_B^C}D_{BC}\left(C_\infty C_{CP} - C_{CP}^2(1-\varphi_{A_{CP}}^+)\right), \quad (44)$$

$$C_{CP}^2\left(\frac{-2n_C D_B}{m_B D_C} + \frac{n_C^C}{m_B^C}\right)$$
$$+ C_{CP}\left(\frac{2C_\infty n_C D_B}{m_B D_C(1-\varphi_{A_{CP}}^+)} - \frac{m_C D_B}{m_B D_C} - m_{CB}^C\right)$$
$$+ g(\varphi_{A_{CP}}^+) - B^* = 0, \quad (45)$$

where $D_{BC} = \frac{D_B}{D_C}$, $m_{CB}^C = \frac{m_C^C}{m_B^C}$, and $B^* = B_E + \frac{T_E - T_E^{AB}}{m_B^C}$. Combining Eqs. (38), (40), and (42), we arrive at the equation

$$a_2(\chi_{SC}^+)^2 + a_1(\chi_{SC}^+) + a_0 = 0, \quad (46)$$

$$\chi_{SC}^+ = \frac{-a_1 \pm \sqrt{a_1^2 - 4a_2 a_0}}{2a_2}, \quad (47)$$

where

$$a_2 = -VL_V D_C + 2C_E^2 V n_C^C k_l - 2C_E^2 V n_C^C k_S - C_E V m_C^C k_l + V C_E m_C^C k_S,$$

$$a_1 = -Vk_l C_\infty (2n_C^C C_E - m_C^C) + C_\infty k_S V(2C_E n_C^C - m_C^C) + k_S G_S D_C + 2C_E^2 V n_C^C k_s - V C_E m_C^C k_S,$$

$$a_0 = -C_\infty k_S V(2C_E n_C^C - m_C^C).$$

From Eqs. (38), (39) and (41), (42), we now determine

$$\varphi^-_{B_{SC}} = B_\infty, \quad (48)$$

$$\varphi^-_{C_{SC}} = C_\infty, \quad (49)$$

$$\varphi^+_{C_{SC}} = 0. \quad (50)$$

$\varphi^+_{A_{CP}}$ and C_{CP} are found from Eqs. (44) and (45), and χ^-_{CP} is then found from Eq. (43) at known C_{CP}. Differential equation (43) can be solved now since $C_{CP} = C(\varphi^+_{A_{CP}})$ is known. Expressions (26), (28), and (29) are combined to obtain equations to find $\varphi^-_{A_{PL}}$, C_1, and B_1. The boundary values on the right of the solid phase–cotectic zone boundary are found from distributions (32) in the form $\varphi^+_{ASC} = \varphi_A\left(\chi^+_{SC}\right)$ and $\varphi^+_{BSC} = \varphi_B\left(\chi^+_{SC}\right)$. Moreover, distributions (32) also determine the boundary fractions of the solid phase of components A and B φ^-_{ACP}, φ^-_{BCP} on the left of the boundary between the cotectic and the main mushy zones, $\varphi^-_{ACP} = \varphi_A\left(\chi^-_{CP}\right)$ and $\varphi^-_{BCP} = \varphi_B\left(\chi^-_{CP}\right)$.

INTERDENDRITIC SPACING

In some practical problems, the determination of the impurity concentration in a solid phase is reduced to measuring the interdendritic spacing and calculating the concentration at the boundary with the solid phase. In our case, the impurity concentration is exactly known as a function of the spatial variable. The interdendritic spacing can be analytically determined. To this end, we write the following equation, which relates these two parameters [28]:

$$\lambda = \sqrt{\frac{2\pi\rho}{0.86\dfrac{\partial(\varphi_A + \varphi_B)}{\partial y}}}. \quad (51)$$

Here, ρ is the radius of curvature that corresponds to stable dendrite growth and is specified by the criterion [6, 29, 30]

$$\frac{2d_0 D_T}{\rho^2 V_d} = \sigma_0 \beta^{7/4}\left[\frac{1}{\left(1 + a_1\sqrt{\beta}P_g\right)^2} + \frac{1}{\left(1 + a_2\sqrt{\beta}P_g\, D_T/D_C\right)^2}\frac{2m_C^C C_i(1-k_0)D_T}{(Q/c_P)\,D_C}\right], \quad (52)$$

where

$$C_i = \frac{C_{CP}}{1 - (1-k_0)\exp\left(P_g\dfrac{D_T}{D_C}\right)P_g\dfrac{D_T}{D_C}I_C(\infty)}, \quad (53)$$

$$I_C(\eta) = \int_1^\eta \exp\left[-P_g\frac{D_T}{D_C}h\right]\frac{dh}{\sqrt{h}}, \quad (54)$$

$a_2 = \sqrt{2}a_1 \approx 0.505\sqrt{\sigma_0}$ and σ_0 are constants to be experimentally determined, d_0 is the capillary length, V_d is the dendrite tip velocity, β is the increase parameter, m_C^C is the slope of liquidus, C_i is the impurity concentration on the dendrite surface, k_0 is the impurity distribution coefficient, Q is the latent heat per unit volume of the solid phase, c_p is the heat capacity, D_T is the thermal conductivity, D_C is the diffusion coefficient, and P_g is the Peclet number.

Combining Eqs. (51)–(54), we can find function $\lambda(P_g)$ in an explicit form.

CONCLUSIONS

A new analytical method was developed to solve the heat-and-mass transfer problem in a ternary system. This method has all limiting transitions to the formulations of the problem studied earlier. The dependences of the impurity concentrations and the fractions of solid and liquid phases were obtained for the case of a linear liquidus equation. The influence of the quadratic term in the liquidus equation on a phase diagram was studied.

Figure 2 shows the effect of coefficient n on the deviation of the liquidus equation from a linear dependence. The small deviations from a linear function at a fixed impurity concentration in the mushy zone can change the temperature by several degrees Celsius. It should be noted that such deviations often take place in practice. As follows from Fig. 2, temperature tends to decrease when n decreases and tends to increase when n increases.

Figure 3 shows the distributions of the fractions of the solid and liquid phases over the entire phase transition zone, which consists of the cotectic and the main two-phase zones. The fraction of the solid substance of component A (φ_A), which undergoes a phase transition in regions I and II, decreases monotonically in the phase transition region. However, the fraction of the solid substance of component B (φ_B), which undergoes a phase transition only in region I, decreases only in the cotectic mushy zone. The length

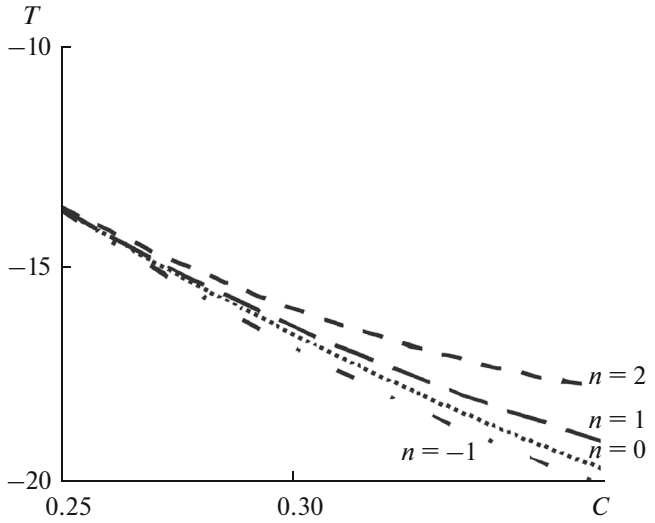

Fig. 2. Effect of coefficient n on the deviation of the liquidus equation from a linear function. Temperature T is measured in Celsius.

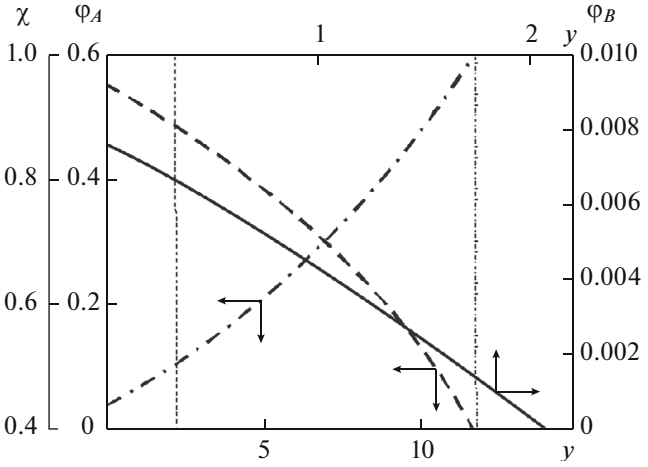

Fig. 3. Fractions of (solid and dashed lines) solid phase and (dot-and-dash line) liquid phase vs. spatial coordinate. Cotectic zone, main zone, and liquid phase are located in regions I, II, and III (regions are indicated by vertical lines for the lower axis), respectively. The thermophysical parameters of the system to be calculated are given in the table (y is measured in centimeters).

of cotectic region I is smaller than the length of the main phase-transition region (region II). According to these dependences, the fraction of the liquid phase χ increases monotonically in the entire phase-transition region (regions I and II). This fraction is determined by the fractions of solid phase φ_A and φ_B in region I and only by fraction φ_A in region II. Therefore, as function $\varphi_A(x)$, distribution $\chi(x)$ also has an inflection point in the main mushy zone. Our calculations demonstrate that the fractions of the solid and liquid phases at the boundaries between regions I and II and regions II and III are continuous (they are discontinuous only at the solid phase–cotectic zone boundary).

Figure 4 depicts the impurity concentration distributions over the entire phase transition region. The basic impurity component have a concentration $C(x)$ and decreases monotonically in regions I and II due to the rejection of the impurity by the solid phase growing in the system. In contrast to this dependence (which has traditional behavior), the concentration of the second component $B(x)$ increases in the cotectic region, intersects the boundary between regions I and II, reaches its maximum in the main mushy zone, and then decreases in this zone and the liquid phase and tends toward initial concentration B_∞. This, at first glance unusual, behavior of impurity concentration $B(x)$ is explained by the fact that component B undergoes a phase transition in region I, which results in a decrease in the concentration near the solid phase–cotectic region boundary. Note that analogous behavior of impurity concentration $B(x)$ was obtained during an analysis of nonstationary self-similar solidification in [3–7]. However, the maximum in those works was found at the boundary of regions I and II. The shift of the maximum to region II is caused by the fact that approximate Scheil impurity diffusion equations (equations without diffusion terms) were used in [3–7]. Therefore, the shift of the maximum toward the main mushy zone is explained by the effect of the diffusion transport of impurity $B(x)$ in a real ternary system.

Note that the influence of coefficient n from the liquidus equation is also visible in Figs. 3 and 4: the behavior of curves did not change, but the mushy zone length increased significantly as compared to the case

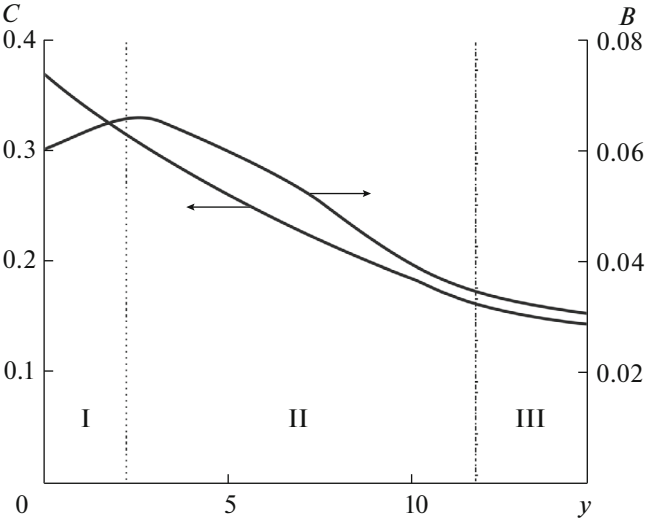

Fig. 4. Concentrations of impurities C and B vs. spatial coordinate $y = z - Vt$. The designations and the calculation parameters correspond to Fig. 2. δ_C = 2.168 cm and δ = 11.803 cm (y is measured in centimeters).

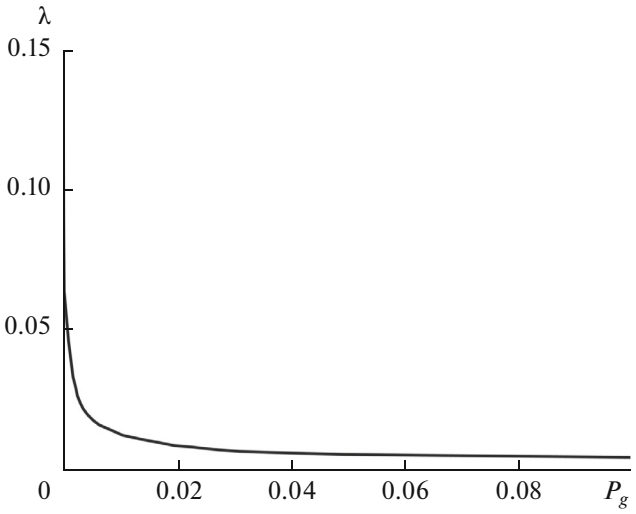

Fig. 5. Interdendritic spacing λ (measured in centimeters) vs. Peclet number P_g. The thermophysical properties of the system are given in the table.

Calculation parameters of the ternary H_2O–KNO_3–$NaNO_3$ system (B and C correspond to $NaNO_3$ and KNO_3, respectively)

B_E	0.06
C_E	0.37
B_E^{AB}	0.10
B_∞	0.035
C_∞	0.152
T_E (°C)	–19
T_E^{AB} (°C)	–5
T_M(°C)	0
κ ($cm^2\ s^{-1}$)	1.1×10^{-3}
D_C ($cm^2\ s^{-1}$)	4.94×10^{-6}
D_B ($cm^2\ s^{-1}$)	4.94×10^{-6}
L_V/k_S (s °C cm^{-2})	1.52×10^5
k_L/k_S	0.25
k_S	5.3×10^{-3}
G_S (°C cm^{-1})	1
k_0	0
σ_0	2.1
β	0.195
D_T ($cm^2\ s^{-1}$)	5×10^{-9}
G_L (°C cm^{-1})	0.5
Q/c_P (°C)	805

of a linear liquidus equation. In addition, the curves elongated.

Figure 5 shows interdendritic spacing λ versus Peclet number P_g. The interdendritic spacing is seen to decrease with increasing P_g. This behavior agrees with the well-known experimental data from [31, 32] and the theory developed in [33].

The main result of this work is the conclusion that even a small deviation of the liquidus equation from a linear function can lead to a substantial change in the solidification parameters.

ACKNOWLEDGMENTS

This work was supported in part by the Russian Foundation for Basic Research, project no. 16-08-00932.

REFERENCES

1. V. T. Borisov, *Theory of the Two-Phase Zone in a Metal Ingot* (Metallurgiya, Moscow, 1987).
2. Yu. A. Buyevich, D. V. Alexandrov, and V. V. Mansurov, *Macrokinetics of Crystallization* (Begell House, New York, 2001).
3. D. V. Alexandrov, "On the theory of the formation of the two-phase concentration-supercooling region," Physics Doklady **48**, 481–486 (2003).
4. D. V. Alexandrov and I. G. Nizovtseva, "Nucleation and particle growth with fluctuating rates at the intermediate stage of phase transitions in metastable systems," Proc. Roy. Soc. A **470**, 20130647 (2014).
5. D. V. Alexandrov and A. P. Malygin, "Nucleation kinetics and crystal growth with fluctuating rates at the intermediate stage of phase transitions," Modell. Simul. Mater. Sci. Eng. **22**, 015003 (2014).
6. D. V. Alexandrov and P. K. Galenko, "Dendrite growth under forced convection: analysis methods and experimental tests," Physics–Uspekhi **57**, 771–786 (2014).
7. J. Gao, M. Han, A. Kao, K. Pericleous, D. V. Alexandrov, and P. K. Galenko, "Dendritic growth velocities in an undercooled melt of pure nickel under static magnetic fields: a test of theory with convection," Acta Mater. **103**, 184–191 (2016).
8. A. C. Fowler, "The formation of freckles in binary alloys," IMA J. Appl. Math. **35**, 159–174 (1985).
9. R. N. Hills, D. E. Loper, and P. H. Roberts, "A thermodynamically consistent model of a mushy zone," Q. J. Mech. Appl. Math. **36**, 505–539 (1983).
10. M. G. Worster, "Solidification of an alloy from a cooled boundary," J. Fluid Mech. **167**, 481–501 (1986).
11. V. T. Borisov, "Crystallization of a binary alloy at retained stability," Dokl. Akad. Nauk SSSR **136**, 583–586 (1961).
12. V. T. Borisov and Yu. E. Matveev, "Determination of temperatures at the beginning of the two-phase zone in binary alloys," Fiz. Met. Metalloved. **13**, 456–470 (1962).

13. D. V. Alexandrov, "Solidification with a quasiequilibrium mushy region: analytical solution of nonlinear model," J. Crystal Growth **222**, 816–821 (2001).
14. D. V. Alexandrov, "Solidification with a quasiequilibrium two-phase zone," Acta Mater. **49**, 759–764 (2001).
15. D. V. Alexandrov and D. L. Aseev, "One-dimensional solidification of an alloy with a mushy zone: thermodiffusion and temperature-dependent diffusivity," J. Fluid Mech. **527**, 57–66 (2005).
16. D. V. Alexandrov and D. L. Aseev, "Directional solidification with a two-phase zone: thermodiffusion and temperature-dependent diffusivity," Comp. Mater. Sci. **37**, 1–6 (2006).
17. D. V. Alexandrov and A. P. Malygin, "Analytical description of seawater crystallization in ice fissures and their influence on heat exchange between the ocean and the atmosphere," **441**, 1407–1411 (2006).
18. D. V. Alexandrov, D. L. Aseev, I. G. Nizovtseva, H.-N. Huang, and D. Lee, "Nonlinear dynamics of directional solidification with a mushy layer. Analytic solutions of the problem," Int. J. Heat Mass Transfer **50**, 3616–3623 (2007).
19. D. V. Alexandrov, I. G. Nizovtseva, A. P. Malygin, H.-N. Huang, and D. Lee, "Unidirectional solidification of binary melts from a cooled boundary: analytical solutions of a nonlinear diffusion-limited problem," J. Phys.: Condens. Matter **20**, 114105 (2008).
20. D. M. Anderson, "A model for diffusion-controlled solidification of ternary alloys in mushy layers," J. Fluid Mech. **483**, 165–197 (2003).
21. A. Aitta, H. E. Huppert, and M. G. Worster, "Diffusion-controlled solidification of a ternary melt from a cooled boundary," J. Fluid Mech. **432**, 201–217 (2001).
22. D. V. Alexandrov and A. P. Malygin, "The steady-state solidification scenario of ternary systems: exact analytical solution of nonlinear model," Int. J. Heat Mass Transfer **55**, 3755–3762 (2012).
23. D. V. Alexandrov and A. A. Ivanov, "Solidification of a ternary melt from a cooled boundary, or nonlinear dynamics of mushy layers," Int. J. Heat Mass Transfer **52**, 4807–4811 (2009).
24. D. V. Alexandrov and A. A. Ivanov, "The Stefan problem of solidification of ternary systems in the presence of moving phase transition regions," J. Exper. Theor. Phys. **108**, 821–829 (2009).
25. A. S. Jordan, "The liquidus surfaces of ternary systems involving compound semiconductors: II. Calculation of the liquidus isotherms and component partial pressures in the Ga–As–Zn and Ga–P–Zn systems," Metall. Trans. **2**, 1965–1970 (1971).
26. D. V. Alexandrov, I. V. Rakhmatullina, and A. P. Malygin, "On the theory of solidification with a two-phase concentration supercooling zone," Russ. Metall. (Metally), No. 8, 745–750 (2010).
27. D. M. Herlach and D. M. Matson, *Solidification of Containerless Undercooled Melts* (Wiley, Weinheim, 2012).
28. R. Deguen, A. Alboussière, and D. Brito, "On the existence and structure of a mush at the inner core boundary of the Earth," Phys. Earth Planet. Inter. **164**, 36–49 (2007).
29. D. V. Alexadrov and P. K. Galenko, "Selection criterion of stable dendritic growth at arbitrary Peclet numbers with convection," Phys. Rev. E **87**, 062403 (2013).
30. D. V. Alexadrov and P. K. Galenko, "Thermo-solutal and kinetic regimes of an anisotropic dendrite growing under forced convective flow," Phys. Chem. Chem. Phys. **17**, 19149–19161 (2015).
31. K. Somboonsuk, J. T. Mason, and R. Trivedi, "Interdendritic spacing: Part I. Experimental studies," Metall. Trans. A **15**, 967–975 (1984).
32. R. Trivedi, "Interdendritic spacing: Part II. A comparison of theory and experiment," Metall. Trans. A **15**, 977–982 (1984).
33. D. V. Alexandrov and A. V. Britousova, "Interdendritic spacing in growth processes with a mushy layer," AIP Conf. Proc. **1648**, 850101 (2015).

Translated by K. Shakhlevich